Assessing Cyclone-Induced Landscape Transformation in the Coastal Town of Diu, India: Insights from Cyclone Tauktae using Sentinel-2

Sharmistha Bhowmik[1]*, Kandarp Parmar[1], Lakhan Jain[2], Janak Joshi[3], Bindu Bhatt[1]
[1]Department of Geography, Faculty of Science, The Maharaja Sayajirao University of Baroda, Vadodara, Gujarat, India
[2]PMCoE Rajiv Gandhi Government PG College, Mandsaur, Madhya Pradesh, India
[3]Vadodara Smart City Development Limited, Vadodara, Gujarat, India
*Corresponding Author: sharmib24031988@gmail.com

(Received on 03 January 2025; In final form on 04 April 2026)

DOI: *https://doi.org/10.58825/jog.2026.20.1.213*

Abstract: Natural disasters occur often around the world, and their incidence and intensity appear to be increasing in recent years. The disasters, like cyclones and floods, usually cause vital loss of life, large-scale economic and social impacts, environmental damages, and drastic changes in land use and land cover (LULC). Cyclones can cause devastating impacts, including strong winds, heavy rainfall, storm surges, and flooding. The aftermath includes infrastructure damage, loss of life, displacement of communities, and ecological disruptions. Studying the impact of cyclones on LULC is crucial to inform the design and implementation of natural vegetation management, identify threatened habitats, prevent and/or counter environmental threats, and enhance conservation efforts and offers valuable insights for disaster preparedness, infrastructure planning, and climate resilience. Understanding and forecasting the consequences of climate change is critical to support the work of planners and decision makers. The coastal wetland of Diu, with numerous creeks and channels, is associated with shoals and vast tidal flats and has one of the richest zones for mangroves along the west coast of India. The study portrays the occurrence of a TAUKTAE, a super cyclonic storm of the 21st century, to land in Gujarat, Saurashtra, and Diu, the most-hit, which was formed over the Arabian Sea. The research uses Sentinel 2A to derive different indices such as NDVI, used in mapping vegetation change, and NDBI (Normalized Difference Built-up Index) to detect changes based on the spectral response of built-up areas for the pre- and post-cyclone Tauktae periods. This study can enhance understanding of vulnerability and aid in formulating strategies to mitigate cyclone impacts, ensuring sustainable development in the region.

Keywords: Tauktae, NDVI, NDBI, Sentinel, LULC, Disaster management

1. Introduction

The Indian subcontinent is vulnerable to landslides, drought, tropical cyclones (TCs) along the coast, earthquakes in the Himalayas, and floods brought on by heavy precipitation (Kannaujiya et al. 2024). In India, the coastal regions are susceptible to extreme weather induced by tropical cyclones (Rajeevan et al. 2013; Murakami et al. 2017; Poulose et al. 2020; Chakravarty et al. 2021; Mishra et al. 2021). Both the east and west coasts experience cyclones in the pre-monsoon (May–June) and post-monsoon (October–November) seasons (Kumar et al. 2024).

A cyclone is an extreme meteorological occurrence brought on by disturbances in the vicinity of a low-pressure zone over bodies of water. Winds spiral in a snake-like coil around the center of this low-pressure zone and pick up speed. In the northern hemisphere, these winds circulate anticlockwise, and in the southern hemisphere, clockwise. It is referred to as a tropical cyclone when it forms over tropical waters (NDMA India, 2021).

The frequency and intensity of tropical cyclones have increased markedly since the 1970s (Bhatia et al. 2019; Emanuel, 2005; Guzman and Jiang, 2021), and the trend is expected to continue in the future (Knutson et al. 2010). Climate change is predicted to facilitate this continuing trend of cyclone severity, and economic damages are expected to double by 2100 (Mendelsohn et al. 2012).

In terms of human casualties and financial harm, tropical cyclones pose a serious threat to tropical coastal areas. India's wide coastal region is particularly at risk from severe tropical cyclones (Subrahmanyam et al. 2002).

This is especially true in May and October when tropical cyclones occur most frequently. Before the onset of the southwest monsoon in June, cyclonic storms also form over the southeastern Arabian Sea. Only approximately 7% of tropical storms originate in the North Indian Ocean, which includes the Bay of Bengal (BOB) and the Arabian Sea. The ratio of occurrence of tropical cyclones over the Arabian Sea is about 4:1 in comparison to the Bay of Bengal (Byju and Prasanna Kumar, 2011; Dube et al. 1997).

The frequency and intensity of cyclones in the BOB are five times higher than in the Arabian Sea because of the warmer sea surface temperature (SST) in the BOB (Singh et al. 2000, Alam, et al. 2015), which is one of the favourable conditions that sustain TCs. It may be remarked that, over the BOB, the highest SSTs are recorded during May and November. Half of the TCs did not sustain over the Arabian Sea because of the colder SST than in other adjacent regions (Evan et al. 2011). However, during 2014–2019, nine extremely severe cyclones were recorded in the Arabian Sea (i.e., the Nilofar cyclone in 2014; the Mega and Chapala cyclones in 2015; the Luban and Mekunu cyclones in 2018; and the Vayu, Hika, Kyar, and Maha cyclones in 2019) (IMD 2020, Krishnan 2020).

Analysis of cyclone impacts in coastal areas in India has been reported by Patra et al. (2013), Lotliker et al. (2014), Murty et al. (2014), Sebastian and Behera (2015), Yu et al. (2015), Chaudhuri et al. (2014), Singh et al. (2016), Thakur et al. (2018), and Parida et al. (2018). Studies in a similar direction are conducted for different cyclones visiting the Bay of Bengal, viz., Cyclone Fani (Mishra et al. 2021); Gaja Cyclone-Induced Changes to Plantation Crops using NDVI Differencing and Classification Methods (Veeramani, 2020); and Amphan in 2020 in India and Bangladesh.

Cyclone Tauktae has affected more than half of India and badly hit all states on India's west coast. It has made 2021 the third year in a row to experience a cyclone that originated in the Arabian Sea during the pre-monsoon season (April-June). It also represents the third year in a row that a cyclone has made landfall somewhere near India's west coast, following Cyclones Vayu and Nisarga in 2019 and 2020, respectively. SSTs in the Arabian Sea before the onset of cyclonic storms are currently between 1.2 and 1.4 degrees Celsius higher than in past decades, according to the most recent studies. In comparison to the baseline temperatures between 1981 and 2010, the SST in the Arabian Sea increased by 0.36 degrees Celsius, according to a 2019 report from the IMD. Clearly defined, the likelihood of more cyclones forming increases as the ocean warms (Times Now Digital, 2021).

2. Study Area

Diu is in the union territory of Dadra and Nagar Haveli and Daman and Diu. The beach town famed for its Portuguese-style architecture is a pale shadow of its past glory. Never before in the last several decades have Diu witnessed such a devastation left behind by Cyclone Tauktae that roared into Gujarat from this coast. Diu, an island of 38.8 sq km with a 17 km shoreline, is adjacent to the Port of Veraval and is separated from the Saurashtra peninsula's southernmost point by a small channel that passes through a swamp. The island falls between the latitudes of 20°44'34" and 20°42'00" north and the longitudes of 71°00'24" and 70°52'26" east of Greenwich. The island is flanked on three sides by the Arabian Sea and in the north by two districts of Gujarat, Gir-Somnath and Amreli. The north of the island, adjacent to Gujarat, consists of tidal marshes and salt pans, while the south coast is built of magnificent limestone cliffs, rocky coves, and pleasant, quiet sandy beaches. Diu extends 13.8 kilometers in an east-west direction and only 4.6 km in a north-south direction. Figure 1. Shows the location map of Diu Island.

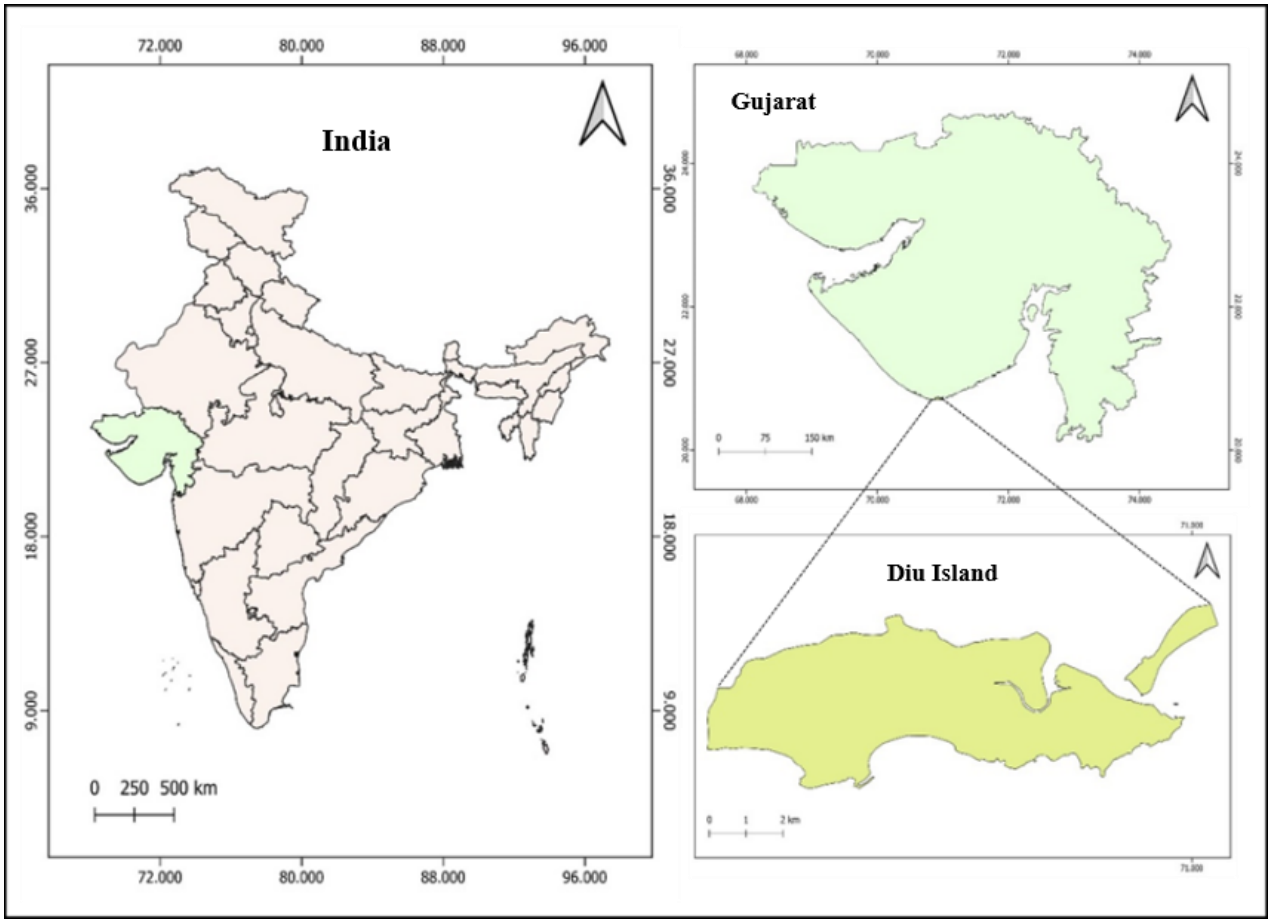

Figure 1: Map of Study Area

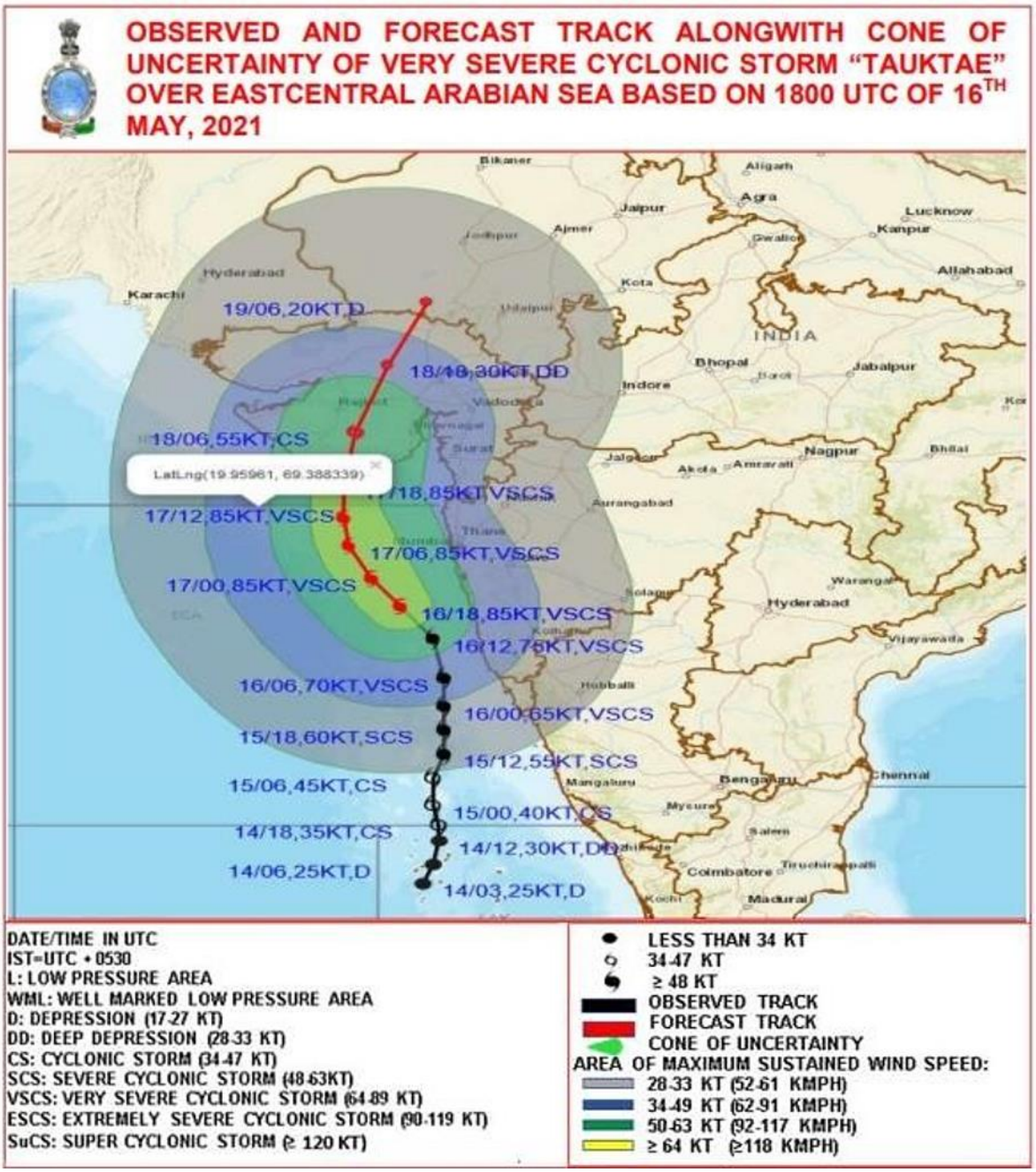

Figure 2: Track and Cone of Uncertainty of Cyclone "Tauktae" (Source: IMD, 2021)

Diu experiences cool, dry weather all year round and receives about 60 cm of rainfall annually. Despite being showered by the southwest monsoon rainfall from June to September, the island does not get as much rain as the area around South Gujarat. The island gets a mild winter (daytime peaks of 20°C, evening lows of 15°C) during December and January. The pre-monsoon months (March to May) are warm (a maximum of 36 degrees Celsius), although the temperature does not rise abnormally. The island comes under the Very High Damage Risk Zone-B (Vb=50 m/s) as per the Wind and Cyclone Vulnerability Map of India. As per the Flood Hazard Map of India, the probable surge height of this region is 4.5 m (NDMA, 2016). The climate of this region is extremely warm and humid, with an average annual rainfall of 1500 mm. The coastal wetland of Diu, with numerous creeks and channels, is associated with shoals and vast tidal flats and has one of the richest zones for mangroves along the west coast of India.

2.1 Synoptic Portrayal of Tauktae

Figure 2. Depicts the track and cone of uncertainty of cyclone Tauktae. On May 13, 2021, early in the morning (08:30 IST/03:00 UTC), a low-pressure region developed over the southeast Arabian Sea and the nearby Lakshadweep area. It was visible as a low-pressure area that evening (1730 IST/1200 UTC on May 13), centered over the Lakshadweep region and the nearby southeast Arabian Sea. On May 14, 2021, early in the morning (0830 IST), it condensed into a depression over the Lakshadweep region owing to favourable environmental circumstances. On May 14, around 1430 IST/0900 UTC, it became a deep depression over the Lakshadweep area and the nearby southeast and east central Arabian Sea, and then at 2330 IST/1800 UTC, it became cyclonic storm "TAUKTAE"

over the exact area (IMD, 2021). The name given to the tropical cyclone Tauktae (pronounced "Tau'Te") comes from Myanmar, India's neighbouring country, and it symbolizes the gecko, a particularly noisy lizard found in the Burmese region (Kumar et al. 2024). Tauktae reached its peak strength by early May 17, when it had become an exceptionally strong cyclonic storm. At 2000–2300 hours IST on May 17, 2021, it reached a marginally unfavorable environment, weakened gradually, and passed the Saurashtra coast close to latitude 20.8°N and longitude 71.1°E, about 20 km northeast of Diu, with maximum sustained winds gusting to 185 kmph with a wind speed of 160–170 kmph (IMD, 2021). It lost strength later that day when it went through an eye-wall replacement cycle (the creation of a new eye to replace the old one that reduces the cyclone's intensity). In Gujarat's Gir-Somnath district, it eventually made landfall. Cyclone Tauktae started to gradually lose strength on May 19 as it shrank into a clearly defined low-pressure area as a result of its interaction with land. The Brown Ocean effect from the Gulf of Khambhat and the Gulf of Kutch, which occurs when a tropical cyclone continues to intensify even after impacting land, is the cause of Tauktae's somewhat slower fading. IMD verified that cyclone Tauktae was affected by western disturbances, which caused it to move slowly over the coast and continue to receive a sufficient amount of moisture from the sea (Verma Kopal and Gupta Kumar Anil, 2021).

On May 17, 2021, Tauktae, an exceptionally strong tropical cyclone, made landfall in Gujarat, India. Maximum sustained winds of 100 knots (185 km/h) and gusts of up to 125 knots (230 km/h), which are equal to category 3 or 4 hurricanes, were recorded by the US Joint Typhoon Warning Center as Tauktae got closer to land (Kannaujiya et al. 2024). Strong winds of such intensity can snap trees, topple power lines, damage homes, and drive a storm surge of up to 3 meters onto the Indian coast, causing significant destruction in some areas (Kannaujiya et al. 2024).

3. Data Source and Methodology

The schematic layout of the methodology has been presented in Figure 3.

3.1 Sentinel-2 L2A data

Sentinel-2 L2A was assessed from Copernicus Sentinel Data and Service Information (ESA, 2021). Two satellites make up the Sentinel-2 Multi-spectral Instrument (MSI), which can observe the Earth at spatial resolutions of 10, 20, and 60 meters (Abdi, 2020; Drusch et al. 2012). 4 visible bands, 6 near-infrared bands, and 3 short-wave infrared bands make up Sentinel-2 L2A's total of 13 bands (Sentinel Hub, 2021). Sentinel-2's fundamental goal is to provide high-resolution satellite data for monitoring land cover and use, climate change, and disasters (Malenovský et al. 2012; Phiri et al. 2020). Forest monitoring, land cover change detection, and natural disaster management are all supported by frequent revisit time (10 days closest to the equator with one satellite and 5 days with two satellites) (Nguyen et al. 2020; Vuolo et al. 2016).

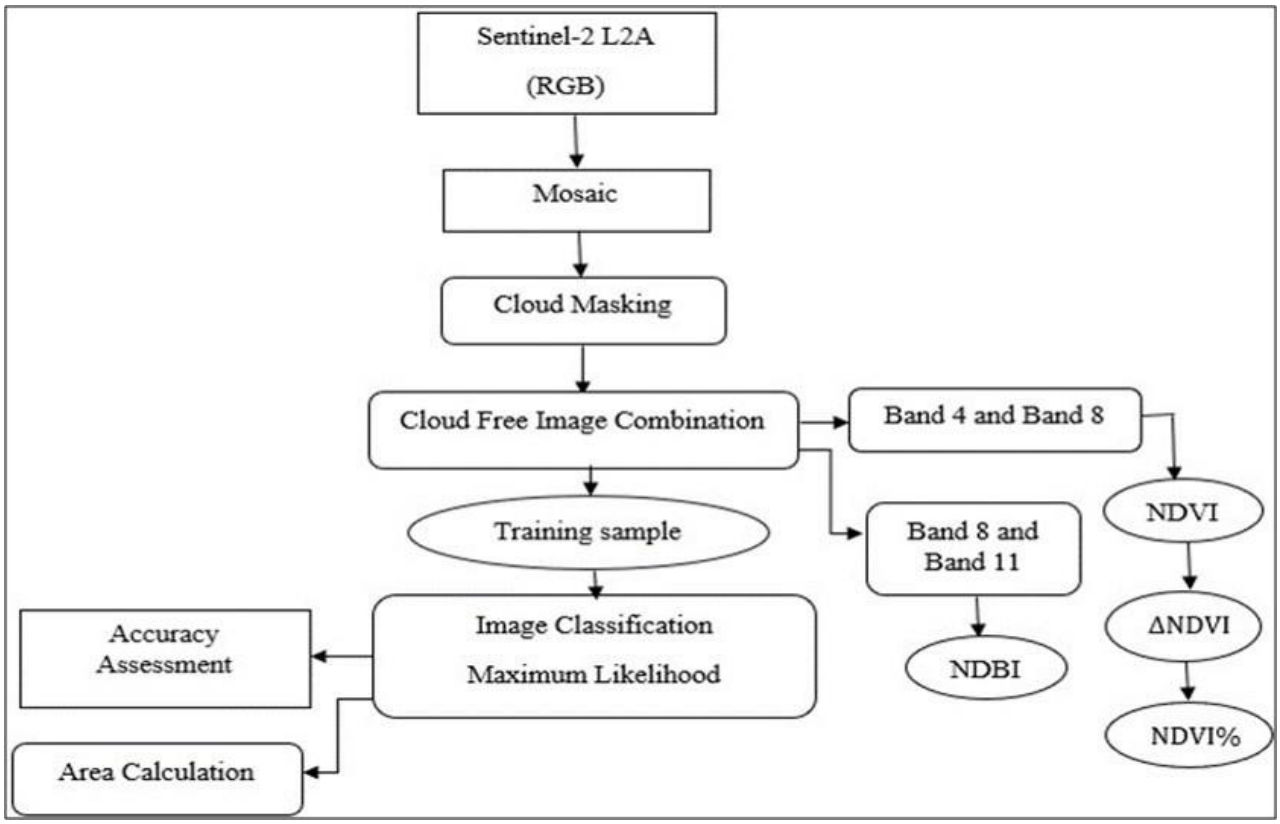

Figure 3: Methodology Applied in the Study

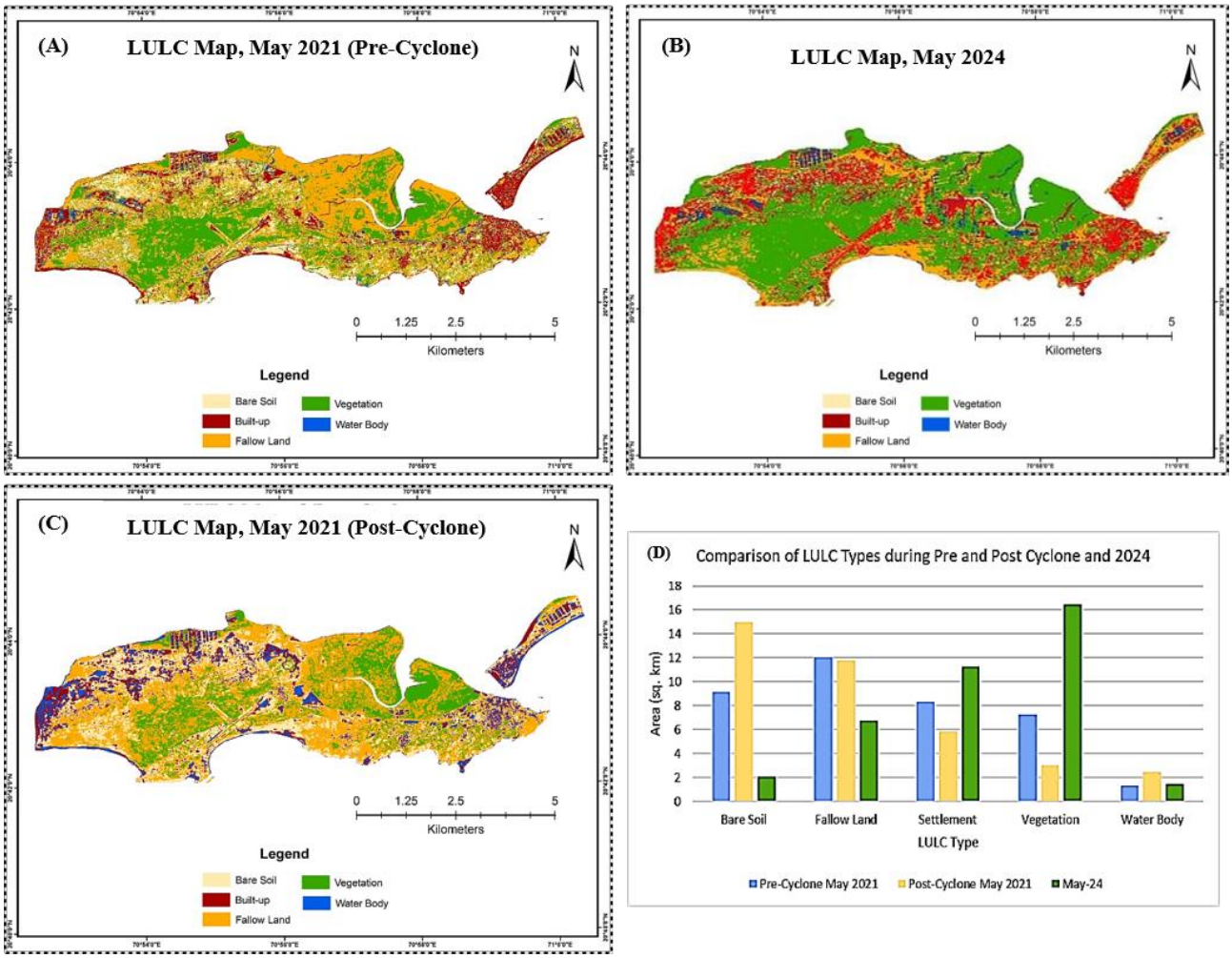

Figure 4: (A) LULC Map of Pre-Cyclone (B) LULC Map of Post-Cyclone (C) LULC Map of May 2024 (D) Comparison of Pre, Post and May 2024

3.2 Method

3.2.1 Derivation of LULC

Using the cloud with less than 10% satellite images acquired on May 15, 2021, and May 25, 2021, the authors have classified and analysed the various LULC classes. Additionally, authors have included 2024 satellite data to make analysis more up-to-date and give more detailed temporal comparison. This addition helps the readers to see the immediate pre- and post-event changes that are related to cyclone Tauktae and the long-term landscape responses in Diu, which enhances the relevance and robustness of the study.

Table 1: Value Range of LULC Classes

Value Range	LULC category
0.00 - 0.08	Waterbody
0.08 - 0.20	Built-up
0.15 - 0.35	Bare soil
0.20 - 0.40	Fallow land
0.35 - 0.80	Vegetation

The Maximum Likelihood Classifier (MLC) algorithm of supervised classification was carried out for this investigation by using ARCGIS 10.2. Only supervised classification was carried out for this investigation. In supervised classification, each pixel in the image is given the cover type to which its spectral signature is most similar after the user creates the spectral signatures of well-known categories, such as urban and forest (Eastman and J.R., 2003; Rwanga and Ndambuki, 2017). Table 1 shows the value range of LULC classes for the study area, LULC categorization was then divided into classes such as bare soil, fallow land, vegetation, settlement, and water body using training samples.

Applying the following formulas, accuracy assessment for LULC classification was completed:

$$\text{Producer's Accuracy (\%)} = \left(\frac{X_{kk}}{X_{+k}}\right) * 100 \quad (1)$$

$$\text{User's Accuracy (\%)} = (X\_kk/X\_(k+)\ ) * 100\% \quad (2)$$

The total number of pixels in row "k" and column "k" is represented by the symbol X_{kk}, total samples in a row "k" are represented by X_{k+}. The total samples are represented

by X_{+k} in column "k" of the error matrix (Vivekananda et al. 2021).

$$\text{Overall Accuracy (T)} = \frac{\Sigma D_{ii}}{N} \quad (3)$$

Kappa Co-efficient (K)

$$K = \frac{N\Sigma_{i-1}^{r} x_{ii} - \Sigma_{i-1}^{r}(x_{i+} * x_{+i})}{N^2 - \Sigma_{i-1}^{r}(x_{i+} * x_{+i})} \quad (4)$$

Where N is the total number of pixels, r is the number of rows in the matrix, xii is the number of observations in row I and column I and xi+ and x+i, respectively, are the marginals for row I and column i. The range of the kappa coefficient is 0 to 1, with 1 denoting perfect agreement and 0 denoting no better agreement than would be anticipated by chance (Das and Das, 2021).

3.2.2 Derivation of NDVI

The Normalized Difference Vegetation Index (NDVI) is a numerical indicator that uses the visible and near-infrared bands of the electromagnetic spectrum (Bhowmik and Bhatt, 2023; Parmar and Bhatt, 2025) and is adopted to analyse remote sensing measurements and assess whether the target being observed contains live green vegetation or not.

The Normalized Difference Vegetation Index (NDVI) is generally used to measure vegetation density and its health status (level of photosynthetic activity) and is less affected by topographic factors and illumination (Zhang et al. 2013).

The ground surface feature's spectral reflectance is the basis for the NDVI index (Singh Ravi Prakash et al. 2016). It can promote vegetation by deducting one spectral band from another because of the unequal reflectance of objects over various wavelength ranges (Fatemi and Narangifard, 2019). It is a ratio that results from the straightforward difference between NIR and red reflectance and is normalized by the equation (Mishra and Singh, 2019; Tucker, 1979).

$$\text{NDVI} = \frac{NIR - RED}{NIR + RED} \quad (5)$$

NDVI from Sentinel-2 is calculated by the equation described by (Strashok Oleksandra et al. 2022).

$$\text{NDVI} = \text{Index (B8, B4)} = \frac{B8 - B4}{B8 + B4} \quad (6)$$

3.2.3 Derivation of NDBI

For environmental monitoring, the Normalized Difference Built-up Index (NDBI) is another crucial urban climate indicator (Koko et al. 2021; Rousta et al. 2018). This provides details on the geographic extent of built-up regions and impervious surfaces, making it an efficient method for mapping and assessing land-uses (Koko et al. 2021). NDBI can be calculated by the formula used by (Chen et al. 2020):

$$\text{NDBI} = \frac{\boldsymbol{\rho}\text{SWIR1} - \boldsymbol{\rho}\text{NIR}}{\boldsymbol{\rho}\text{SWIR1} + \boldsymbol{\rho}\text{NIR}} \quad (7)$$

After the abovementioned processing, the areas of change can be located by dividing the NDVI image for one period by the NDVI image for the other (Cakir et al. 2006; Hu and Smith, 2018). The NDVI image from before the Tauktae was subtracted from the image after the Tauktae using map algebra, which is a cell- by-cell procedure. The following equation calculates the NDVI difference:

$$\Delta NDVI = NDVI_{pre} - NDVI_{post} \quad (8)$$

where "ΔNDVI" represents the difference in NDVI prior to landfall and after landfall." NDVIpre" refers to the NDVI image taken before Tauktae makes landfall and "NDVIpost" refers to the NDVI image taken after Tauktae makes landfall.

The following equation was used to compute the relative vegetation change activity following Tauktae ("NDVI%") (Charrua et al. 2021):

$$NDVI\% = \frac{\Delta NDVI}{NDVI_{pre}} * 100 \quad (9)$$

4. Results

4.1 Diu's Spatial Variability on Land Use and Land Cover

Figure 4(A), Figure 4(B) and Figure 4(C) shows LULC Map of pre-cyclone, post-cyclone and May 2024, while Figure 4(D) provides Comparison of Pre, Post and May 2024. For examining the validity of the land cover maps, a quantitative accuracy evaluation was performed and efficiency was carefully examined with the aid of Google Earth Engine (GEE). In Table 2, the contents of the metadata are noted. Overall accuracy calculated was 95.11%, and the kappa coefficient was 93.60% for pre. For the post, overall accuracy was 93%, and the kappa coefficient was 92.57%. Land cover classes during the pre- and post-cyclone periods of Tauktae in 2021 and the same time period in 2024 reveal significant shifts. After the cyclone in 2021, bare soil significantly increased from 9.15 sq. km to 14.95 sq. km, indicating soil exposure likely due to vegetation loss. As a result of the cyclone's effect on vegetation, the amount of vegetation covers drastically decreased from 7.24 square kms to 3.01 square kms. The total area of settlements decreased from 8.31 square kms to 5.83 square kms, possibly as a result of infrastructural damage. However, by 2024, settlement areas had increased to 11.30 sq. km, suggesting urban development, but vegetation had greatly risen to 16.45 sq. km, suggesting environmental recovery.

4.2 Spatial Distribution of NDVI

The max NDVI value before Tauktae was 0.83, and the min value was -0.18. The max value after Tauktae decreased to 0.76, and the min value went down to NDVI from the pre-period to the post-period changed from 0.63 to 0.49. Hence, it can be concluded that Tauktae had an

Table 2. Mean NDVI of Each Class for Pre and Post cyclone and NDVI Change

LULC Class	Mean NDVI (pre cyclone)	Mean NDVI (post cyclone)	ΔNDVI	NDVI%
Vegetation	0.67	0.36	-0.31	-46.26
Settlement	0.29	0.18	-0.11	-37.93
Bare soil	0.30	0.22	-0.08	-26.67
Fallow land	0.51	0.33	-0.18	-33.96
Water body	0.19	0.15	-0.04	-21.05

adverse effect on vegetation. The shift in NDVI value is greatest where vegetation was present before Tauktae's arrival, as shown in Figure 5. The change of NDVI value was moderate and low where there were settlements and barren land, and it was least in the area occupied by water bodies. Hence, it can be stated that Tauktae had an adverse effect on vegetation. Areas occupied by dense vegetation and where there existed tall trees were more affected than areas occupied by sparse vegetation or small agricultural lands. ΔNDVI on various LULC classes were also calculated along with NDVI%, and their metadata are provided in Table 4. Figure 5.depicts NDVI Map of (A) Pre-Cyclone (B) Post-Cyclone (C) May 2024.

4.3 Spatial Distribution of NDBI

As along with vegetation, settlement was also affected by the cyclone Tauktae, so through NDBI, the rate of destruction of the settlement area was calculated. The max value of NDBI before the arrival of Tauktae was 0.72, and the min value was -0.36. The max value of NDBI decreased to 0.35, and the min value decreased to -0.53 after the arrival of Tauktae. The mean value of NDBI before the arrival of Tauktae was 0.45 and decreased to 0.21 after the arrival of Tauktae.

In 2021, the post-cyclone NDVI reduced sharply from 0.63 (pre-cyclone) to 0.49, showing that cyclone-induced damage had caused a loss of vegetation. On the contrary, the 2024 NDVI was higher at 0.68, indicating that the vegetation cover had improved with time. In 2021, after cyclone Tauktae, NDBI values, which measure the

intensity of built-up areas, also indicate a substantial reduction, going from 0.45 to 0.21, most likely as a result of infrastructure destruction. The NDBI increased to 0.48 in 2024, indicating potential urban development and recovery in the years that followed. These patterns indicate the cyclone's immediate impact on infrastructure and vegetation in 2021 as well as the recovery or changes observed in 2024 (Table 2).

From the above Table 3, it is clear that change in NDVI (NDVI) is max in vegetation, followed by fallow land and settlement. There have been very minimal changes to bare soil and water bodies. The NDVI% is lower in vegetation, followed by settlement and fallow land. Bare soil and water bodies carry the higher value. Thus, it can be concluded that maximum destruction was done to vegetation, and water bodies were least affected.

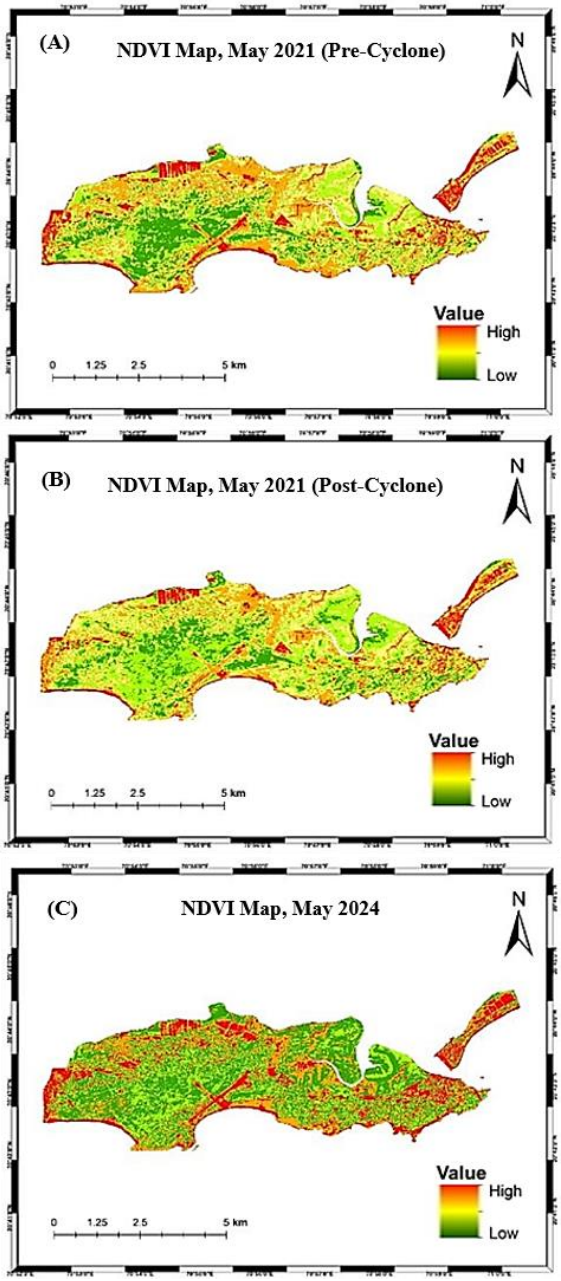

Figure 5: NDVI Map of (A) Pre-Cyclone (B) Post-Cyclone (C) May 2024

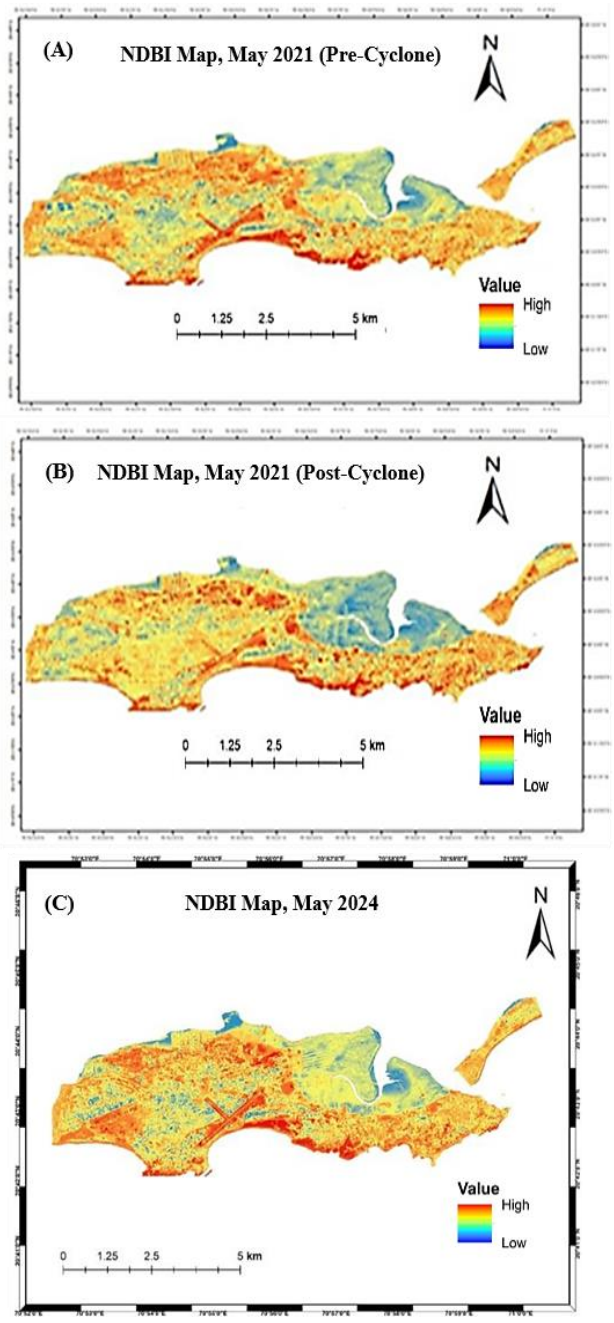

Figure 6: NDBI Map of (A) Pre-Cyclone (B) Post-Cyclone (C) May 2024

It is to be noted that lower damage is indicated by a higher NDVI% (Charrua et al. 2021). Figure 6 shows NDBI Map of (A) Pe-Cyclone (B) Post-Cyclone (C) May 2024.

5. Discussion Damage Analysis

5.1 Effect of Tauktae Attributing to Land Use Land Cover Change

From the above metadata on LULC, it can be stated that due to the arrival of Tauktae, vegetation has decreased by 58.42% of the area. In regions near the Saurashtra shore, standing crops are estimated to have suffered 90% destruction. Summer crops, along with mangoes and pulses, were affected in Junagadh. Likewise, settlement also decreased by 29.84% in area. According to Mishra Lalatendu (2021), Gujarat and Diu bear the bulk of the damage, along with many homes, ports, and electrical power substations, in addition to the electric poles and trees. About 2.5 lakh homes were impacted by the storm, which further worsened damage to kutcha homes. Concrete houses haven't sustained a lot of damage. In 2018, the centrally managed Diu district established a reputation for being self-sufficient in terms of its energy requirements, and that too by relying on solar energy. The solar farm in Malala Village, next to the Gangeshwar Mahadev temple, has been severely damaged by Cyclone Tauktae (Singh and Ankit, 2021). Fallow land was also affected by the change in area, which was negligible; it decreased by 2%. The area of the bare land on the other increased as it replaced the area occupied especially by vegetation and settlement. Thus, the area of bare land increased by 63.39%. The area occupied by the water body also increased by 88.46% due to heavy rainfall. It is evident from the above Figure 7 that Tauktae's arrival caused the greatest reduction in the number of pixels of vegetation, followed by settlement and fallow land. On the other hand, throughout the same period, the number of pixels representing water bodies and bare land increased.

There are some notable changes in LULC, such as vegetation to bare soil (4.75 km²), indicating loss of vegetation that was likely related to the high winds and storm effects of the cyclone. There are transitions like bare soil to fallow land (2.49 km²) and bare soil to vegetation (2.35 km²) that show local recovery or surface modification on the land after the occurrence. Particularly, Built-up to Waterbody (1.50 km²) indicates potential flooding or short-term waterlogging of lands at low coastal zones. Other smaller transitions, such as built-up to fallow land and waterbody to bare soil, also indicate short-term changes in the patterns of land cover. In general, the findings emphasize the effects of cyclones on the landscape disruption, vegetation degradation, and local flooding impacts on the coastal setting of Diu (Table 4).

Table 3: Maximum, Minimum and Mean NDVI and NDBI Value of Pre and Post Cyclone and with May 2024

	Max	Min	Mean
Pre-Cyclone NDVI	0.83	-0.18	0.63
Post-Cyclone NDVI	0.76	-0.20	0.49
2024 NDVI	0.79	-0.16	0.68
Pre-Cyclone NDBI	0.72	-0.36	0.45
Post-Cyclone NDBI	0.35	-0.53	0.21
2024 NDBI	0.78	-0.41	0.48

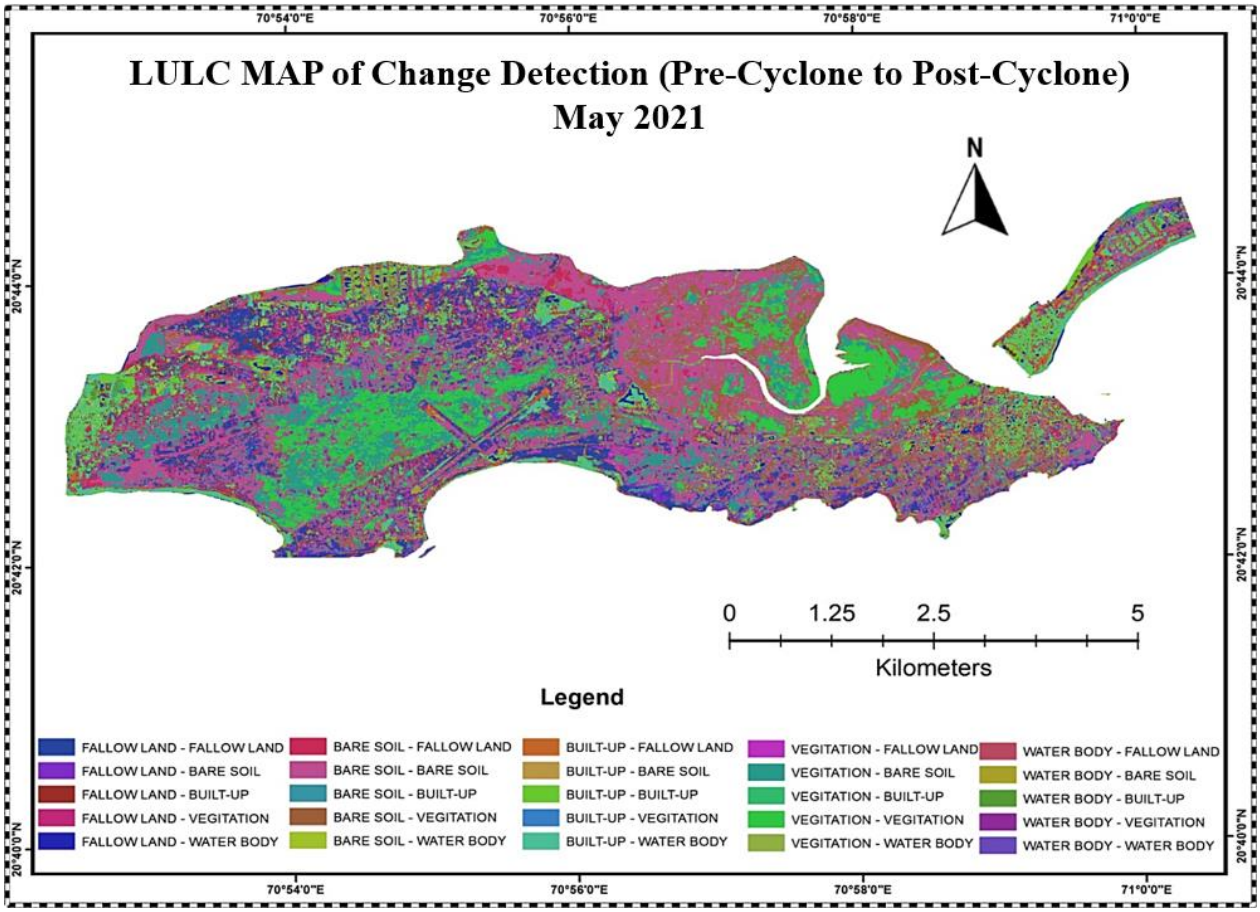

Figure 7: LULC Change Detection

Table 4: LULC Class Wise Change Detection

LULC Class change (From - To)	Change in Area (Sq. km)
Bare Soil - Bare Soil	7.58
Vegetation - BARE SOIL	4.75
Vegetation - Vegetation	3.46
Fallow Land - Fallow Land	3.18
Bare Soil - Fallow Land	2.49
Bare Soil - Vegetation	2.35
Built-up - Built-up	2.02
Built-up - Waterbody	1.50
Fallow Land - Bare Soil	1.17
Built-up - Fallow Land	1.08
Vegetation - Fallow Land	0.86
Bare Soil - Built-up	0.77
Waterbody - Fallow Land	0.52
Waterbody - Bare Soil	0.47
Fallow Land - Built-up	0.47
Fallow Land - Waterbody	0.43
Bare Soil - Waterbody	0.35
Waterbody - Built-up	0.19
Vegetation - Built-up	0.12
Built-up - Bare Soil	0.11
Waterbody - Waterbody	0.08
Vegetation - Waterbody	0.05
Fallow Land - Vegetation	0.01
Waterbody - Vegetation	0.01
Built-up - Vegetation	0.00

6. Conclusions

One of the most devastating natural catastrophes that affect many nations across the world is a tropical cyclone, which results in significant loss of life, agricultural loss, and loss of property in coastal areas. In this study, the harm caused on the LULC by Cyclone Tauktae, which struck Diu in May 2021, is evaluated. The study's findings had been obtained using remote sensing and GIS. In order to map and evaluate the hazard-prone areas, local knowledge combined with GIS and RS techniques at the catastrophe identification stage is a great instrument for managing cyclone disasters and developing regional planning. Storm surge is the main danger posed by cyclone Tauktae, especially in the vicinity of the area of landfall. The analysis revealed that vegetation suffered the most harm, followed by habitation, as Tauktae's track was located just 20 kilometers from Diu. This work is only to demonstrate the temporal changes in the LULC and the method used to assess the changes between two periods. The high-

resolution data is necessary to enhance the current work. It is also necessary to have the cloud-free data immediately after the cyclone to have a better understanding. Cyclone and land use and land cover (LULC) change can have significant impacts on the human population, and if both coexist, the consequences for people and the surrounding environment may be severe.

Acknowledgements
The authors express sincere gratitude for the financial assistance provided by the University Grants Commission (UGC) under the scheme SJSGC/JRF to Sharmistha Bhowmik and NET/JRF to Kandarp Parmar. We also like to thank USGS for providing data and Google Earth Engine for providing their data processing capabilities.

Data Availability Statement
The manuscript includes all datasets generated or analyzed during the course of this research.

Disclosure Statement
The authors declare no competing interests.

References

Abdi, A. M. 2020. "Land Cover and Land Use Classification Performance of Machine Learning Algorithms in a Boreal Landscape Using Sentinel-2 Data." *GIScience and Remote Sensing* 57(1). https://doi.org/10.1080/15481603.2019.1650447

Alam, E., and D. Dominey-Howes. 2015. "A New Catalogue of Tropical Cyclones of the Northern Bay of Bengal and the Distribution and Effects of Selected Landfalling Events in Bangladesh." *International Journal of Climatology* 35:801–835.

Bhatia, K. T., G. A. Vecchi, T. R. Knutson, H. Murakami, J. Kossin, K. W. Dixon, and C. E. Whitlock. 2019. "Author Correction: Recent Increases in Tropical Cyclone Intensification Rates." *Nature Communications* 10(1). https://doi.org/10.1038/s41467-019-11922-2

Bhowmik, S., and B. Bhatt. 2023. "Spatiotemporal Analysis of Land Surface Temperature Owing to NDVI: A Case Study of Vadodara District, Gujarat." *Journal of Geomatics* 17(1):48–57. https://doi.org/10.58825/jog.2023.17.1.83

Byju, P., and S. Prasanna Kumar. 2011. "Physical and Biological Response of the Arabian Sea to Tropical Cyclone Phyan and Its Implications." *Marine Environmental Research* 71(5). https://doi.org/10.1016/j.marenvres.2011.02.008

Cakir, H. I., S. Khorram, and S. A. C. Nelson. 2006. "Correspondence Analysis for Detecting Land Cover Change." *Remote Sensing of Environment* 102(3–4). https://doi.org/10.1016/j.rse.2006.02.023

Chakravarty, K., N. Arun, P. Yadav, R. Bhangale, P. Murugavel, V. P. Kanawade, et al. 2021. "Characteristics of Precipitation Microphysics during Tropical Cyclone Nisarga (2020) as Observed over the Orographic Region of Western Ghats in the Indian Sub-Continent." *Atmospheric Research* 264:105861.

Charrua, A. B., R. Padmanaban, P. Cabral, S. Bandeira, and M. M. Romeiras. 2021. "Impacts of the Tropical Cyclone Idai in Mozambique: A Multi-Temporal Landsat Satellite Imagery Analysis." *Remote Sensing* 13(2). https://doi.org/10.3390/rs13020201

Chaudhuri, S., D. Dutta, S. Goswami, and A. Middey. 2014. "Track and Intensity Forecast of Tropical Cyclones Using Neural Networks." *Meteorological Applications* 22(3):563–575.

Chen, J., S. Chen, C. Yang, L. He, M. Hou, and T. Shi. 2020. "A Comparative Study of Impervious Surface Extraction Using Sentinel-2 Imagery." *European Journal of Remote Sensing* 53(1). https://doi.org/10.1080/22797254.2020.1820383

Das, M., and A. Das. 2021. "Assessing the Impact of Master Plan on the Dynamicity and Resilience of Forest Cover Change: A Study on Adina Deer Park (Forest), West Bengal, India." *GeoJournal* 86(6). https://doi.org/10.1007/s10708-020-10213-4

Drusch, M., U. del Bello, S. Carlier, O. Colin, V. Fernandez, F. Gascon, B. Hoersch, et al. 2012. "Sentinel-2: ESA's Optical High-Resolution Mission for GMES Operational Services." *Remote Sensing of Environment* 120. https://doi.org/10.1016/j.rse.2011.11.026

Dube, S. K., A. D. Rao, and P. C. Sinha. 1997. "Storm Surge Forecasting in the Bay of Bengal and Arabian Sea." *Mausam* 48(2):283–304. https://doi.org/10.54302/mausam.v48i2.4012

Eastman, J. R. 2003. *Guide to GIS and Image Processing*. Clark University Manual.

Emanuel, K. 2005. "Increasing Destructiveness of Tropical Cyclones over the Past 30 Years." *Nature* 436(7051):686–688. https://doi.org/10.1038/nature03906

ESA. 2021. "Copernicus Open Access Hub." Retrieved (https://scihub.copernicus.eu/).

Evan, A. T., and S. J. Camargo. 2011. "A Climatology of Arabian Sea Cyclonic Storms." *Journal of Climate* 24(1):140–158. https://doi.org/10.1175/2010jcli3611.1

Fatemi, M., and M. Narangifard. 2019. "Monitoring LULC Changes and Its Impact on the LST and NDVI in District 1 of Shiraz City." *Arabian Journal of Geosciences* 12(4). https://doi.org/10.1007/s12517-019-4259-6

Guzman, O., and H. Jiang. 2021. "Global Increase in Tropical Cyclone Rain Rate." *Nature Communications* 12(1). https://doi.org/10.1038/s41467-021-25685-2

Hu, T., and R. B. Smith. 2018. "The Impact of Hurricane Maria on the Vegetation of Dominica and Puerto Rico Using Multispectral Remote Sensing." *Remote Sensing* 10(6). https://doi.org/10.3390/rs10060827

IMD. 2021. "Extremely Severe Cyclonic Storm Tauktae over the Arabian Sea (14th–19th May 2021)." Retrieved (https://internal.imd.gov.in/).

India Meteorological Department (IMD). 2020. *IMD Best Track Report over the Bay of Bengal, Arabian Sea and Land Surface of India*. Retrieved (https://mausam.imd.gov.in/).

Kannaujiya, V. K., A. K. Rai, and S. Malakar. 2024. "Nature and Impact of Extremely Severe Cyclone Tauktae over India." *Discover Oceans* 1(4). https://doi.org/10.1007/s44289-024-00004-x

Knutson, T. R., J. L. McBride, J. Chan, K. Emanuel, G. Holland, C. Landsea, et al. 2010. "Tropical Cyclones and Climate Change." *Nature Geoscience* 3(3):157–163.

Koko, A. F., W. Yue, G. A. Abubakar, A. A. N. Alabsi, and R. Hamed. 2021. "Spatiotemporal Influence of Land Use/Land Cover Change Dynamics on Surface Urban Heat Island." *ISPRS International Journal of Geo-Information* 10(5). https://doi.org/10.3390/ijgi10050272

Krishnan, R., J. Sanjay, C. Gnanaseelan, M. Mujumdar, A. Kulkarni, and S. Chakraborty. 2020. *Assessment of Climate Change over the Indian Region*. Springer Nature.

Kumar, R., P. S. Pippal, A. Chauhan, R. P. Singh, R. Kumar, A. Singh, and J. Singh. 2024. "Dynamics of Land, Ocean, and Atmospheric Parameters Associated with Tauktae Cyclone." *Environmental Science and Pollution Research* 31(8):12561–12576. https://doi.org/10.1007/s11356-023-31659-2

Lotliker, A. A., T. S. Kumar, V. S. Reddem, and S. Nayak. 2014. "Cyclone Phailin Enhanced the Productivity Following Its Passage: Evidence from Satellite Data." *Current Science* 106(3).

Mendelsohn, R., K. Emanuel, S. Chonabayashi, and L. Bakkensen. 2012. "The Impact of Climate Change on Global Tropical Cyclone Damage." *Nature Climate Change* 2(3):205–209.

Mishra, D., and B. N. Singh. 2019. "Derivation of Magnitude of Crop Diversity through NDVI Composite Index Using Sentinel-2 Satellite Imagery." *Journal of the Indian Society of Remote Sensing* 47(5). https://doi.org/10.1007/s12524-019-00951-5

Mishra, M., C. A. G. Santos, R. M. da Silva, N. K. Rana, D. Kar, and N. R. P. M. Lalatendu. 2021. "Gujarat, Diu Bore 65% of the ₹15,000 Crore Estimated Loss Caused by Tauktae: Pushpendra Johari." *The Hindu*. Retrieved (https://www.thehindu.com/business/gujarat-diu-bore-65-of-the-15000-crore-estimated-loss-caused-by-tauktae/article34609334.ece

Murakami, H., G. A. Vecchi, and S. Underwood. 2017. "Increasing Frequency of Extremely Severe Cyclonic Storms over the Arabian Sea." *Nature Climate Change* 7(12):885–889.

Murty, P. L. N., K. G. Sandhya, P. K. Bhaskaran, F. Jose, R. Gayathri, T. M. Balakrishnan Nair, et al. 2014. "A Coupled Hydrodynamic Modeling System for PHAILIN Cyclone." *Coastal Engineering* 93:71–81.

NDMA. 2016. *National Disaster Management Plan*. New Delhi.

NDMA. 2021. "Double Trouble: Cyclone Tauktae and Cyclone Yaas." Retrieved (https://ndma.gov.in/).

Nguyen, H. T. T., T. M. Doan, E. Tomppo, and R. E. McRoberts. 2020. "Land Use/Land Cover Mapping Using Multitemporal Sentinel-2 Imagery." *Remote Sensing* 12(9). https://doi.org/10.3390/rs12091367

Parida, B. R., S. N. Behera, B. Oinam, N. R. Patel, and R. N. Sahoo. 2018. "Investigating Effects of Cyclones Using Remote Sensing." *Remote Sensing Applications: Society and Environment* 10:128–137.

Parmar, K., and B. Bhatt. 2025. "Assessing a Two-Decadal Thermal Landscape Transformation in Expanding City of Vadodara, Gujarat Using MODIS and GEE." *Theoretical and Applied Climatology* 156(7). https://doi.org/10.1007/s00704-025-05578-w

Patra, M., S. Tripathy, and I. Jena. 2013. "Health Hazards by Sea Cyclones in Odisha, the Supercyclone and the Phailin." *Odisha Review* 70(4):30–37.

Phiri, D., M. Simwanda, S. Salekin, V. R. Nyirenda, Y. Murayama, and M. Ranagalage. 2020. "Sentinel-2 Data for Land Cover/Use Mapping: A Review." *Remote Sensing* 12(14). https://doi.org/10.3390/rs12142291

Poulose, J., A. D. Rao, and S. K. Dube. 2020. "Mapping of Cyclone-Induced Extreme Water Levels along Gujarat and Maharashtra Coasts: A Climate Change Perspective." *Climate Dynamics* 55(11):3565–3581.

Rajeevan, M., P. Rohini, K. Niranjan Kumar, J. Srinivasan, and C. K. Unnikrishnan. 2013. "A Study of Vertical Cloud Structure of the Indian Summer Monsoon Using CloudSat Data." *Climate Dynamics* 40(3):637–650.

Rousta, I., M. O. Sarif, R. D. Gupta, H. Olafsson, M. Ranagalage, Y. Murayama, H. Zhang, and T. D. Mushore. 2018. "Spatiotemporal Analysis of Land Use/Land Cover and Its Effects on Surface Urban Heat Island Using Landsat Data: A Case Study of Metropolitan City Tehran (1988–2018)." *Sustainability* 10(12). https://doi.org/10.3390/su10124433

Rwanga, S. S., and J. M. Ndambuki. 2017. "Accuracy Assessment of Land Use/Land Cover Classification Using Remote Sensing and GIS." *International Journal of Geosciences* 8(4). https://doi.org/10.4236/ijg.2017.84033

Sebastian, M., and M. R. Behera. 2015. "Impact of SST on Tropical Cyclones in North Indian Ocean." *Procedia Engineering* 116:1072–1077.

Sentinel Hub. 2021. *Sentinel Hub Documentation*. Retrieved (https://docs.sentinel-hub.com/api/latest/).

Singh, Ankit. 2021. "Four Days after Cyclone Tauktae's Landfall, Diu Still without Power; Mango, Coconut, Banana Crops Flattened in Gujarat." *Gaon Connection*, May 21. Retrieved (https://en.gaonconnection.com/cyclone-tauktae-death-toll-gujarat-maharashtra-diu-crop-damage-farmers-barge-ndrf-navy-modi-vijay-rupani/).

Singh, O. P., T. A. Khan, and M. S. Rahman. 2000. "Changes in the Frequency of Tropical Cyclones over the North Indian Ocean." *Meteorology and Atmospheric Physics* 75:11–20.

Singh, R. P., N. Singh, S. Singh, and S. Mukherjee. 2016. "Normalized Difference Vegetation Index (NDVI) Based Classification to Assess the Change in Land Use/Land

Cover (LULC) in Lower Assam, India." *International Journal of Advanced Remote Sensing and GIS* 5(10):1963–1970. https://doi.org/10.23953/cloud.ijarsg.74

Strashok, O., M. Ziemiańska, and V. Strashok. 2022. "Evaluation and Correlation of Sentinel-2 NDVI and NDMI in Kyiv (2017–2021)." *Journal of Ecological Engineering* 23(9):212–218. https://doi.org/10.12911/22998993/151884

Subrahmanyam, B., K. H. Rao, N. Srinivasa Rao, V. S. N. Murty, and R. J. Sharp. 2002. "Influence of a Tropical Cyclone on Chlorophyll-a Concentration in the Arabian Sea." *Geophysical Research Letters* 29(22). https://doi.org/10.1029/2002GL015892

Thakur, M. K., T. V. L. Kumar, S. Dwivedi, and M. S. Narayanan. 2018. "Rainfall Asymmetry in Tropical Cyclones." *Natural Hazards* 94(2):819–832.

Times Now Digital. 2021. "Cyclone Tauktae Barrels into Gujarat: Why Arabian Sea Is Becoming the New Hotbed of Tropical Storms." May 18. Retrieved (https://www.timesnownews.com/india/article/cyclone-tauktae-barrels-into-gujarat-why-arabian-sea-is-becoming-the-new-hotbed-of-tropical-storms/758379).

Tucker, C. J. 1979. "Red and Photographic Infrared Linear Combinations for Monitoring Vegetation." *Remote Sensing of Environment* 8(2). https://doi.org/10.1016/0034-4257(79)90013-0

Veeramani, S. 2020. "Gaja Cyclone Induced Changes to Plantation Crops Using NDVI Differencing and Classification Methods." *International Journal of Engineering Research & Technology*.

Verma, K., and A. K. Gupta. 2021. "Cyclone Tauktae: Cyclones, Their Impacts and Disaster Risk Management." CAP-RES Climate Adaptive Planning for Resilience & Sustainability Project. Retrieved (https://www.researchgate.net/publication/354450767).

Vivekananda, G. N., R. Swathi, and A. V. L. N. Sujith. 2021. "Multi-Temporal Image Analysis for LULC Classification and Change Detection." *European Journal of Remote Sensing* 54(sup2). https://doi.org/10.1080/22797254.2020.1771215

Vuolo, F., M. Zóltak, C. Pipitone, L. Zappa, H. Wenng, M. Immitzer, M. Weiss, F. Baret, and C. Atzberger. 2016. "Data Service Platform for Sentinel-2 Surface Reflectance and Value-Added Products: System Use and Examples." *Remote Sensing* 8(11). https://doi.org/10.3390/rs8110938

Yu, Z., C. Ji, J. Xu, S. Bao, and J. Qiu. 2015. "Numerical Simulation of Rainstorm Caused by Binary Typhoons." *Atmospheric Research* 166:33–48.

Zhang, Y., J. Gao, L. Liu, Z. Wang, M. Ding, and X. Yang. 2013. "NDVI-Based Vegetation Changes and Their Responses to Climate Change from 1982 to 2011: A Case Study in the Koshi River Basin in the Middle Himalayas." *Global and Planetary Change* 108:139–148. https://doi.org/10.1016/j.gloplacha.2013.06.01